

Article

A Trade-Off between Mechanical Strength and Erosive Wear Resistance in AlSi12CuMgNi Alloy Used to Manufacture Fan Blades for Underground Mines

Florentino Alvarez-Antolin ^{1,*}, Elvira Segurado-Frutos ² , Alejandro González-Pociño ¹, Alberto Cofiño-Villar ¹ and Juan Asensio-Lozano ³ 

¹ Departamento de Ciencia de los Materiales e Ingeniería Metalúrgica, Edificio departamental Este, Universidad de Oviedo, C, Wifredo Ricart s/n- 33204 Gijón (Asturias), Spain; uo204622@uniovi.es (A.G.-P.); uo229780@uniovi.es (A.C.-V.)

² Departamento de Construcción e Ingeniería de Fabricación, Edificio Departamental Oeste, Universidad de Oviedo, C/Pedro Puig Adam s/n- 33204 Gijón (Asturias), Spain; seguradomaria@uniovi.es

³ Departamento de Ciencia de los Materiales e Ingeniería Metalúrgica, Escuela de Ingeniería de Minas, Energía y Materiales, Universidad de Oviedo, C/Independencia 13, 33004 Oviedo (Asturias), Spain; jasensio@uniovi.es

* Correspondence: alvarezflorentino@uniovi.es; Tel.: +34-985-181-949

Received: 21 December 2018; Accepted: 6 March 2019; Published: 11 March 2019



Abstract: The axial fan blades used in underground mines are usually manufactured in AlSi12CuMgNi alloy (EN AC 48000). They must have a high mechanical strength to withstand the stresses resulting from the rotation speed of the rotor and a high resistance to erosive wear caused by suspended particles from underground mining and transport operations. The aim of this paper is to determine the most suitable thermal treatment to simultaneously improve their mechanical strength and erosive wear resistance. To this end, two solution treatments at 525 °C with cooling in water were analysed, as well as several ageing times at 170 °C. The crystalline phases present in the as-cast state were quantified by X-ray diffraction following quenching and different ageing processes. Furthermore, erosion wear resistance was measured by means of compressed air blasting with corundum particles according to ASTM G76 (2004). The highest wear resistance was obtained in the as-cast state using gravity die casting, with the presence of Al₄Cu₂Mg₈Si₇ and Al₃CuNi. This wear resistance was higher than that obtained after the ageing treatment. However, a trade-off between mechanical strength and wear resistance was observed after 12 h ageing, where the hardness obtained exceeded 160 HV and the wear resistance became similar to that obtained in the as-cast state.

Keywords: mine fan blades; Mg₂Si; Al₃Ni; Al₃CuNi; wear; ageing

1. Introduction

Axial fan blades used to ventilate underground mines can be manufactured in aluminium alloys using the gravity die casting technique. These fans enable the supply of fresh air and the extraction of dust and gases resulting from underground operations, such as blasting and the mining, loading, and transport of ore. The required amount of air flows and, hence, the consequent size of these fans depend on three major factors: the concentration of solid airborne particles, the temperature of the air, and the presence of gases which may be flammable or harmful to health [1]. The orientation of the blades and the rotation speed of the rotor have a significant influence on the air flow and the performance of the fan [2]. Besides withstanding the stresses resulting from the rotation speed of the

rotor, the fan blades must present a high resistance to erosive wear caused by suspended particles. Figure 1 shows the blades of a fan subjected to erosive wear. Therefore, the material from which the fan blades are manufactured is required to be light, have high mechanical strength and high wear resistance. Age-hardenable Al–Si alloys can be used for this purpose; these alloys have good castability due to the presence of a eutectic constituent. Al–Si alloys can be alloyed with Cu and Mg to promote their structural hardening by thermal treatment, rendering their use more favourable in applications with high structural requirements [3]. The thermal treatment consists of three stages. In the first stage, a solution treatment is used to dissolve the phases containing Cu and Mg and remove any interdendritic segregation. Spheroidisation and thickening of the eutectic Si also occurs during the first stage [4,5]. In the second stage, the alloy is cooled in water to maintain the aforementioned elements in supersaturated solid solution (quenching). In the third stage, an ageing treatment is used to precipitate intermediate transition phases with a coherent interface from the matrix, thus hardening the alloy. The main intermediate transition phases of these alloys are the β'' (stable β phase: Mg_2Si), θ'' (stable θ phase: $CuAl_2$), and Q'' (stable Q phase: $Al_5Mg_8Si_6Cu_2$) phases [6,7]. However, it should be noted that the presence of the Q phase can be greatly reduced due to the more favourable tendency to form the β phase [8]. The temperatures used in the artificial ageing of these alloys fall within the 150–210 °C range [6]. Following quenching, the material presents a high level of supersaturation and a high density of voids that favour the rapid formation of Guinier–Preston (GP) zones [9]. Transition phases nucleate from these clusters which, despite the existence of elastic stresses induced by the difference in size between the atoms of the solvent and those of the solute, maintain coherent interfaces with the matrix thanks to their nanometric size. Due to the diffusion of the solute atoms, these precipitates can dissolve or increase in size until the interfacial bond is broken, giving rise to incoherent interfaces with the matrix [10]. The increase in strength is conditioned by the size, distribution, and coherence with the matrix of these precipitates [6]. The aim of this paper is to determine the most suitable heat treatment for AlSi12CuMgNi (EN AC 48000) alloy, used in the manufacture of fan blades for underground mines, to achieve high mechanical strength and high erosive wear resistance. This alloy presents excellent castability and can be hardened by means of ageing. The blades manufactured in this alloy are usually used in the as-cast state, however, their strength could be improved by means of adequate solution treatment and ageing. To this end, we studied two solution treatments at 525 °C and several ageing times at 170 °C, and the resulting hardness profiles were determined, specific erosive wear tests were carried out by means of blasting with corundum particles, and the results were correlated with the microstructure of the material.



Figure 1. Mine fan subjected to erosive wear.

2. Materials and Methods

Table 1 shows the chemical composition of the AlSi12CuMgNi material. Samples of this material were subjected to solution treatments at 525 °C, and then cooling in water at 12 °C. The analysed dwell times were 4 and 10 h. Subsequently, several ageing treatments were performed at 170 °C, with different ageing periods between 4 and 30 hours. Vickers Hardness (HV) was obtained under the application of a 0.2 kp load. The results correspond to the mean value obtained from 10 indentations in each specimen. The erosion wear resistance was measured by means of compressed air blasting with corundum particles according to ASTM G76 [11], and applying a pressure of 4 bar, a flow rate of 200 g/min, and a 30° angle of incidence on the sample surfaces. Five repetitions were performed in each test. Metallographic inspection was carried out by means of optical microscopy and scanning electron microscopy (SEM). The optical microscope employed was a NIKON Epiphot 200 (Nikon, Tokyo, Japan) and the scanning electron microscopy employed was a JEOL JSM-5600 (JEOL, Nieuw-Venep, The Netherlands). A semi-quantitative analysis of the main elements present in the precipitated phases was carried out by energy dispersive X-ray (EDX) microanalysis. Preparation of the metallographic samples was carried out via the process of cutting with a SiC disc, cold drawing in plastic resin, roughing on SiC paper using different sizes of abrasive grain, from grit 240 to 600, and, finally, polishing with textile cloths spread with 6 and 1 micron diamond paste and lubricant. X-ray diffraction (XRD) was used to identify and quantify the crystalline phases present in the as-cast state, after the solution treatments at 525 °C and after aging at 170 °C. A Cu ceramic tube located in the fixed primary arm was used as a focus to produce X-rays, operating under 45 kV × 40 mA working conditions. A Ni filter maximized the $K\alpha$ doublet (1.540598–1.544426 Å) of the Cu anode. The recordings were made in continuous mode over the 2θ range between 10 and 140° employing an angular step and count time of 0.0131° and 20 s, respectively. The generalized reference intensity ratio method (RIR) was used to estimate the weight fraction of the crystalline phases by means of semi-quantitative analysis [12,13].

Table 1. Chemical composition range of AlSi12CuMgNi material (% in weight). Rest: Al

%Si	%Fe	%Cu	%Mn	%Mg	%Ni	%Zn	%Ti
11.67	0.14	1.12	0.01	1.3	0.93	0.02	0.12

3. Results

Figure 2 shows the microstructure obtained in the as-cast state (Figure 2a) after solution treatment for 4 h (Figure 2b) and after solution treatment for 10 h (Figure 2c). In Figure 2a, it can be seen that the eutectic is modified [14]. Spheronisation of the Si and an increase in its size can be observed following solution treatment at 525 °C.

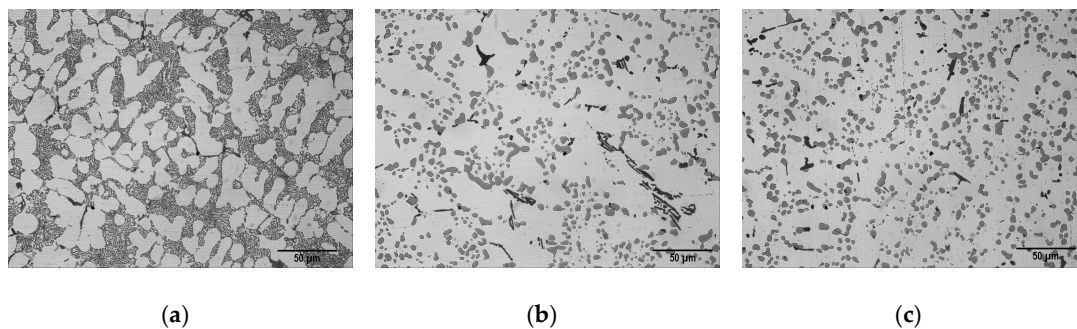


Figure 2. Microstructure of the material obtained by optical microscopy (OM). (a) as-cast state; (b) following a solution treatment at 525 °C for 4 h; (c) following a solution treatment at 525 °C for 10 h.

Figure 3 shows the hardness profiles obtained following the ageing treatments at 170 °C. One of the hardness profiles represents the solution treatment with a dwell time of 4 h (H4) and the other profile represents the solution treatment with a dwell time of 10 h (H10). Error bars indicate the difference between the mean value of the hardness and the maximum and minimum hardness values. The hardness in the as-cast state was 120 HV. After the solution treatments, however, the hardness decreased to 91 HV for the 4 h treatment and to 82 HV for the 10 h treatment. In both cases, there was a marked increase in hardness of up to 154 HV in the first 4 hours of ageing. Hardening then continued at a slower pace until reaching 164 HV, in both cases. When the solution treatment was 4 h the peak hardness was reached after 8 h of ageing. However, when the solution treatment was 10 h the peak hardness was reached after 10–12 h of ageing. In both cases, once the peak hardness was reached, a slight and gradual decrease in hardness occurred.

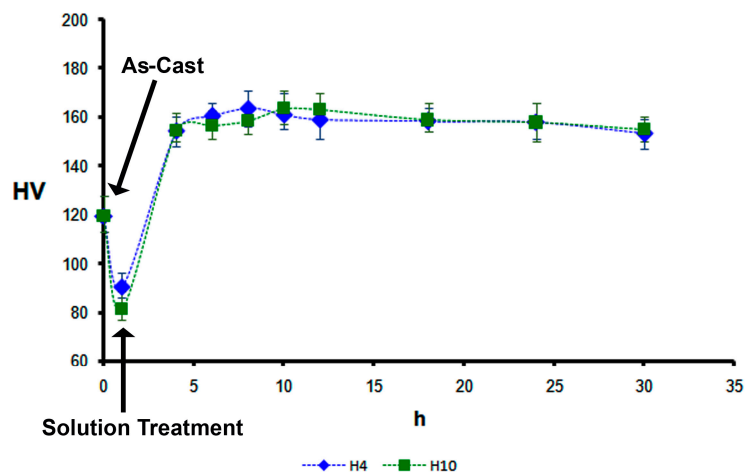


Figure 3. Hardness Vickers (HV) obtained by ageing at 170 °C.

Table 2 shows the crystalline phases present in the as-cast state, after the solution treatments at 525 °C with cooling in water, and after ageing at 170 °C for 8, 12, and 24 h. The thickening of the eutectic Si after solution treatment was confirmed and continued until 8 h of ageing to then undergo constant re-dissolution with increasing ageing times. In the as-cast state, all of the Mg is found in solid solution in the α phase, and the Cu precipitated in phases Al_3CuNi and $\text{Al}_4\text{Cu}_2\text{Mg}_8\text{Si}$. Following the two solution treatments of 4 and 10 h, dissolution of those phases occurred, and precipitation of the Mg_2Si and Al_3Ni phases took place. Phases Al_3CuNi and $\text{Al}_4\text{Cu}_2\text{Mg}_8\text{Si}_7$ are part of a non-equilibrium eutectic. The solution treatment disaggregates the said eutectic constituent, dissolving both phases and allows precipitation of equilibrium phases such as Mg_2Si and Al_3Ni . Furthermore, after solution treatment, the presence of crystalline clusters with a high concentration of Cu atoms is observed which, in minimal percentages (around 0.2%) could have been favourably formed by a high concentration of vacancies after quenching. This high concentration of Cu atoms could coincide with the GP zones [15]. The maximum proportion by weight of these crystalline clusters of Cu is obtained in both solution treatments after 8 h ageing. Subsequently, as ageing continues, these clusters tend to dissolve without the precipitation of any other intermediate transition phases that include Cu or Mg. The maximum percentage of Mg_2Si reaches 2.8% after 10 h solution treatment and 8 h ageing. Figure 4 shows the microstructural evolution of the material from the as-cast state, following the solution treatments at 525 °C, and after ageing at 170 °C for 8, 12, and 24 h. The main precipitated crystalline phases are Si, Al_3Ni , and Mg_2Si . As the ageing times increase, the Al_3Ni , Mg_2Si and Si phases gradually dissolve. During ageing treatment, by diffusion through the matrix, these phases can dissolve and re-precipitate after long periods of time, with delayed kinetics [15]. This could be due to the compositional changes that occur in the alpha matrix. Figure 5 and Table 3 show the results of the semiquantitative analysis, obtained by EDX, on the main crystalline phases present in the as-cast state and after the dissolution treatments.

Table 2. Weight proportion of the crystalline phases present after thermal treatments. Rest: α -phase. (ST: solution treatment).

State	Ageing	%Si	Mg_2Si	Al_3CuNi	Al_3Ni	(Cu)	$\text{Al}_4\text{Cu}_2\text{Mg}_8\text{Si}_7$	Fe_3Si_3	Hardness
As-Cast	-	8.6	-	3.1	-	-	2.1	-	120
	-	9.7	1.5	-	6.4	0.2	-	1.3	91
ST 4 h	8 h	10.2	2.3	-	5.2	0.3	-	0.3	164
	12 h	9.2	1.9	-	4.1	0.2	-	0.2	159
	24 h	6.8	1.3	-	2.9	0.1	-	0.1	158
	-	9.4	1.1	-	6.7	0.2	-	0.2	82
ST 10 h	8 h	9.9	2.8	-	6.2	0.3	-	0.4	158
	12 h	9.1	1.5	-	5.7	0.2	-	0.2	164
	24 h	6.3	1.2	-	2.3	0.1	-	0.1	158

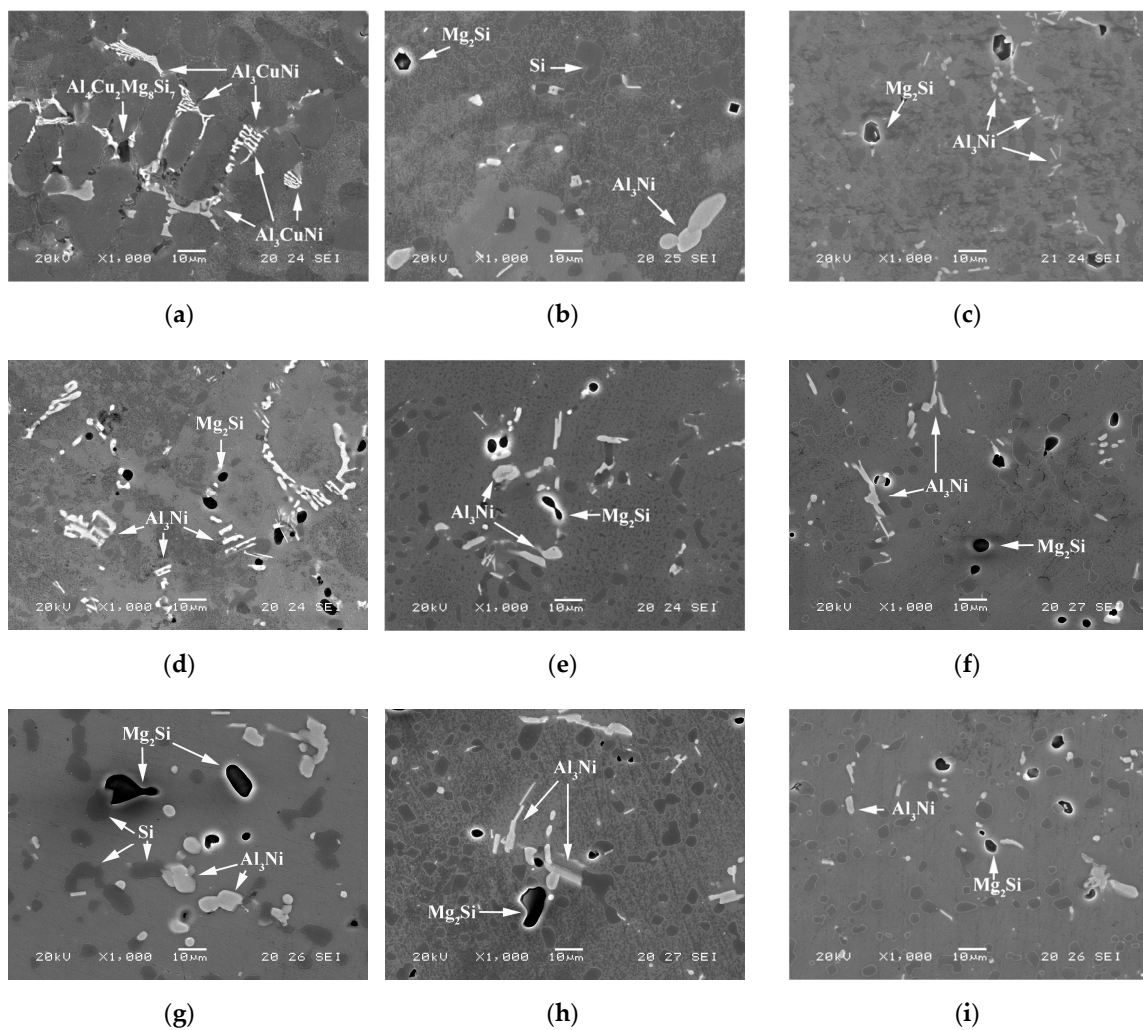


Figure 4. Microstructural evolution. Micrographs obtained by scanning electron microscope (SEM). (a) As-cast; (b) Solution Treatment 525 °C for 4 h; (c) Solution Treatment 525 °C for 4 h, ageing at 170 °C for 8 h; (d) Solution Treatment 525 °C for 4 h, ageing at 170 °C for 12 h; (e) Solution Treatment 525 °C for 4 h, ageing at 170 °C for 24 h; (f) Solution treatment 525 °C for 10 h and quenching; (g) Solution treatment 525 °C for 10 h and quenching, ageing at 170 °C for 8 h; (h) Solution treatment 525 °C for 10 h and quenching, ageing at 170 °C for 12 h; (i) Solution treatment 525 °C for 10 h and quenching, ageing at 170 °C for 24 h.

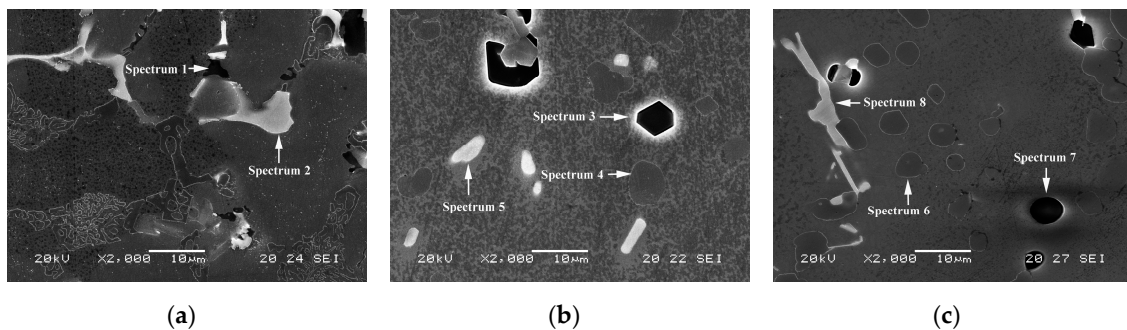


Figure 5. Micrographs obtained by scanning electron microscope (SEM). (a) as-cast state; (b) as-cast following a solution treatment at 525 °C for 4 h; (c) as-cast following a solution treatment at 525 °C for 10 h.

Table 3. Semi-quantitative analysis of the phases indicated in Figure 5, carried out by energy dispersive X-ray (EDX) microanalysis (% in weight).

Spectrum	%Mg	%Al	%Si	%Fe	%Ni	%Cu	State	Possible Phases
1	13.09	56.18	16.84	–	–	13.89	As-cast	$\text{Al}_4\text{Cu}_2\text{Mg}_8\text{Si}_7$
2	–	59.85	–	–	36.04	4.10		Al_3CuNi
3	12.32	39.20	48.47	–	–	–	ST(525°C) 4 h	Mg_2Si
4	–	6.13	93.87	–	–	–		Si
5	–	57.29	2.32	4.63	32.29	3.47	ST(525°C) 10 h	Al_3Ni
6	–	20.59	79.41	–	–	–		Si
7	14.11	26.99	58.90	–	–	–	ST(525°C) 10 h	Mg_2Si
8	–	50.27	2.81	5.74	36.60	4.58		Al_3Ni

Figure 6 shows the average values of the weight losses (mg) per minute observed during the erosion wear tests. It is concluded that the microstructure that performs best against erosive wear corresponds to the as-cast state. Among the aged microstructures, however, those that are aged for 12 h—in which a hardness higher than 160 HV is obtained—perform best against erosive wear. This increase in hardness allows for increased rotor rotation speed and, therefore, the required amount of air flow. The presence of intermetallic compounds like $\text{Al}_4\text{Cu}_2\text{Mg}_8\text{Si}_7$, and especially Al_3CuNi , favour increased wear resistance [16,17]. This wear resistance is superior to that obtained after the precipitation hardening of the α phase.

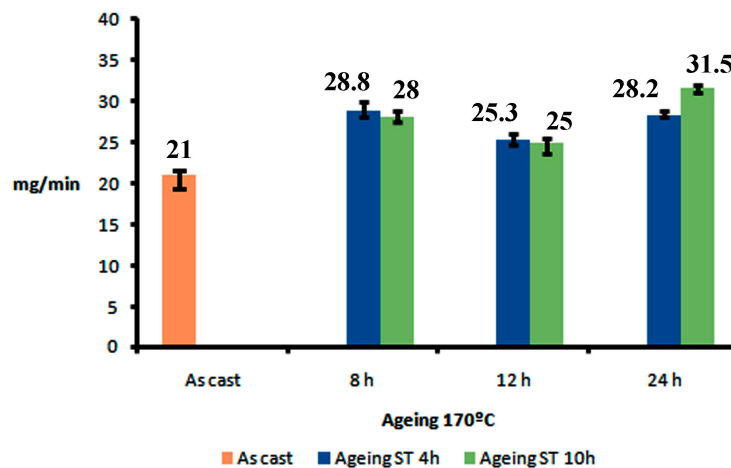


Figure 6. Weight losses suffered during the erosive wear test (ASTM G76) employing compressed air blasting with corundum particles at 4 bar, with a 30° angle of incidence. Five repetitions were performed in each test. The error bars show the distance between the maximum and minimum values and the mean value.

4. Conclusions

Axial fan blades used in underground mining, manufactured from EN AC 48000 alloy by gravity die casting, must have both a high mechanical strength to withstand the forces resulting from the rotation speed of the rotor and a high resistance to erosive wear caused by suspended particles from underground mining and transport operations. The microstructural state that offers greater resistance to erosive wear is the as-cast state using gravity die casting, where the intermetallic Al_3CuNi phase dispersed in α phase has proven to increase the wear resistance to a higher level than that obtained after precipitation hardening. However, the highest mechanical strength is obtained after a 4 h solution treatment at 525 °C with rapid cooling in water and ageing at 170 °C for 8 h. In this case,

the hardness obtained was 164 HV. After 12 h ageing, a trade-off between mechanical strength and wear resistance occurred, where the wear resistance was slightly lower than that obtained in the as cast state, but nevertheless, its hardness was increased to 160 HV.

From the microstructural point of view, it was found that:

1. In the as-cast state, almost all the Mg is found in solid solution in the α phase, while the Cu is found as a precipitate in Al_3CuNi and $\text{Al}_4\text{Cu}_2\text{Mg}_8\text{Si}_7$ phases. These phases are part of a non-equilibrium eutectic. The solution treatment disaggregates said eutectic constituent, dissolving both phases, and allows for the precipitation of equilibrium phases such as Mg_2Si and Al_3Ni .
2. The main precipitated equilibrium phases are Si, Al_3Ni , and Mg_2Si . As the ageing times increase, the Al_3Ni , Mg_2Si and Si phases gradually dissolve by diffusion through the matrix.
3. Following quenching, the formation of crystalline clusters with a high concentration of Cu atoms occurs. These clusters reach their highest weight percentage (0.3%) after 8 h of ageing, and subsequently dissolve with increasing ageing time without the precipitation of intermediate transition phases that include Cu.

Author Contributions: F.A.-A., A.G.-P. and J.A.-L. analysed the microstructure and XRD; E.S.-F., A.G.-P. and A.C.-V. did the heat treatments and determined the hardness profiles; A.G.-P. and A.C.-V. did the wear test; F.A.-A. analysed the data and wrote the paper; J.A.-L. defined the work methodology.

Funding: This research received no external funding.

Acknowledgments: For the realisation of this work, no grants have been received.

Conflicts of Interest: The authors declare no conflict of interest.

References

1. Kazakov, B.P.; Shalimov, A.V.; Kiryakov, A.S. Energy-saving mine ventilation. *J. Min. Sci.* **2013**, *49*, 475–481. [[CrossRef](#)]
2. Pikushchak, E.V.; Minkov, L.L. Method of calculating the aerodynamic efficiency of the axial fan. *J. Math. Mech.* **2016**, 90–101. [[CrossRef](#)] [[PubMed](#)]
3. Pezda, J. Effect of the T6 heat treatment on change of mechanical properties of the AlSi12CuNiMg alloy modified with strontium. *Arch. Metall. Mater.* **2015**, *60*, 627–632. [[CrossRef](#)]
4. Fernandez-Gutierrez, R.; Requena, G.C. The effect of spheroidisation heat treatment on the creep resistance of a cast AlSi12CuMgNi piston alloy. *Mater. Sci. Eng.* **2014**, *598*, 147–153. [[CrossRef](#)]
5. Al Kahtani, S.A.; Doty, H.W.; Samuel, F.H. Combined effect of melt thermal treatment and solution heat treatment on eutectic Si particles in cast Al-Si alloys. *Int. J. Cast Met. Res.* **2014**, *27*, 38–48. [[CrossRef](#)]
6. Sjolander, E.; Seifeddine, S. The heat treatment of Al-Si-Cu-Mg casting alloys. *J. Mater. Process. Technol.* **2010**, *210*, 1249–1259. [[CrossRef](#)]
7. Eskin, D.G. Decomposition of supersaturated solid solutions in Al-Cu-Mg-Si alloys. *J. Mater. Sci.* **2003**, *38*, 279–290. [[CrossRef](#)]
8. Pan, X.; Morral, J.E.; Brody, H.D. Predicting the Q-Phase in Al-Cu-Mg-Si Alloys. *J. Phase Equilib. Diffus.* **2010**, *31*, 144–148. [[CrossRef](#)]
9. Bastow, T.J.; Hill, A.J. Guinier-Preston and Guinier-Preston-Bagaryatsky zone reversion in Al-Cu-Mg alloys studied by NMR. *Res. Innov. Technol.* **2006**, 519–521, 1385–1390. [[CrossRef](#)]
10. Hayoune, A.; Shabestari, S.G.; Hamana, D. Study on the Structural Evolution During Non Isothermal Aging of an Al-Cu-Mg-Si Alloy by Means of Thermal Analysis. *Trans. Indian Inst. Met.* **2016**, *69*, 1529–1535. [[CrossRef](#)]
11. Vishwas, D.K.; Chandrappa, C.N.; Venkatesh, S. Study On Erosion Behaviour Of Hybrid Aluminium Composite. In Proceedings of the 1st International Conference on Design, Materials and Manufacture (ICDEM), Surathkal, India, 29–31 January 2018.
12. Chung, F.H. Quantitative interpretation of X-Ray-Diffraction patterns of mixtures. Adiabatic principle of X-Ray-Diffraction analysis of mixtures. *J. Appl. Crystallogr.* **1974**, *7*, 526–531. [[CrossRef](#)]

13. Davis, B.L. Semiquantitative XRD analysis with the aid of reference intensity ratio estimates. *Powder Diffr.* **1998**, *13*, 185–187. [[CrossRef](#)]
14. Pero-Sanz, J.A. *Ciencia e Ingeniería de Materiales*, 4th ed.; Dossat 2000: Madrid, Spain, 2000; p. 676.
15. Ashby, M.; Jones, D. *Engineering Materials 2*, 2nd ed.; Butterworth Heinemann: Oxford, UK, 1998; Volume 2.
16. Yang, C.W.; Chang, Y.H.; Lui, T.S.; Chen, L.H. Effects of friction stir processing and artificial peak aging on erosion resistance of Al-11Si-4Cu-2Ni-0.7Mg cast alloy. *Mater. Des.* **2012**, *40*, 163–170. [[CrossRef](#)]
17. Farkoosh, A.R.; Javidani, M.; Hoseini, M.; Larouche, D.; Pekguleryuz, M. Phase formation in as-solidified and heat-treated Al-Si-Cu-Mg-Ni alloys: Thermodynamic assessment and experimental investigation for alloy design. *J. Alloy. Comp.* **2013**, *551*, 596–606. [[CrossRef](#)]



© 2019 by the authors. Licensee MDPI, Basel, Switzerland. This article is an open access article distributed under the terms and conditions of the Creative Commons Attribution (CC BY) license (<http://creativecommons.org/licenses/by/4.0/>).